



Photoluminescence properties of Co^{2+} -doped ZnO nanocrystals

Petra Lommens^a, Philippe F. Smet^b, Celso de Mello Donega^c, Andries Meijerink^c,
Luc Piraux^d, Sebastien Michotte^d, Stefan Mátéfi-Tempfi^d,
Dirk Poelman^b, Zeger Hens^{a,*}

^aPhysical Chemistry Laboratory, Ghent University, Krijgslaan 281-S12, B-9000 Ghent, Belgium

^bDepartment of Solid State Science, Ghent University, Krijgslaan 281-S1, B-9000 Ghent, Belgium

^cDebye Institute, Utrecht University, PO Box 80000, 3508 TA Utrecht, The Netherlands

^dUnité de Physico-Chimie et de Physique des Matériaux, Place Croix du Sud 1, 1348 Louvain-la-Neuve, Belgium

Received 8 June 2005

Available online 19 October 2005

Abstract

We performed photoluminescence experiments on colloidal, Co^{2+} -doped ZnO nanocrystals in order to study the electronic properties of Co^{2+} in a ZnO host. Room temperature measurements showed, next to the ZnO exciton and trap emission, an additional emission related to the Co^{2+} dopant. The spectral position and width of this emission does not depend on particle size or Co^{2+} concentration. At 8 K, a series of ZnO bulk phonon replicas appear on the Co^{2+} -emission band. We conclude that Co^{2+} ions are strongly localized in the ZnO host, making the formation of a Co^{2+} *d*-band unlikely. Magnetic measurements revealed a paramagnetic behaviour.

© 2005 Elsevier B.V. All rights reserved.

PACS: 75.50.Pp; 78.55.Et; 61.46.+w

Keywords: Diluted magnetic semiconductors; Photoluminescence; ZnO

1. Introduction

Semiconductors can be made ferromagnetic by partially replacing non-magnetic elements by

magnetic transition metal ions (TM). Due to their spin-transport properties, these so-called diluted magnetic semiconductors (DMS) hold the promise of many interesting spintronic device applications [1,2]. The most extensively studied DMS is most likely $\text{Ga}_{1-x}\text{Mn}_x\text{As}$ [3,4]. Here, the ferromagnetic exchange interaction coupling the Mn spins is mediated by free holes. However, the low

*Corresponding author. Tel.: +32 9 264 48 63;
fax: +32 9 264 49 71.

E-mail address: Zeger.Hens@UGent.be (Z. Hens).

ferromagnetic ordering temperatures ($T_C \leq 110$ K) are still limiting the practical use of this material. Research is now being focused on the search for materials with critical temperatures ranging above room temperature. Theory not only predicts high temperature ferromagnetism in arsenides but also in TM-doped semiconducting oxides [5,6]. Based upon ab initio calculations, it was suggested that ferromagnetic ordering in TM-doped ZnO is due to the occurrence of a spin-split, partially filled TM *d*-band [6,7]. Several authors reported room temperature magnetic hysteresis loops for ZnO doped with Mn, Co or Ni, although others did not find any evidence of ferromagnetism [8–11]. Recent results indicate that the presence of free electron carriers plays an important role in enhancing the ferromagnetism [2,12,13].

We performed luminescence experiments on strongly confined Co^{2+} -doped ZnO nanocrystals (Co:ZnO) to probe the electronic structure of Co^{2+} in the ZnO host, in casu, the assumed formation of a Co^{2+} related *d*-band within the band gap of the ZnO. The advantage of working with nanocrystals instead of bulk materials or thin layers lies in the fact that due to quantum confinement, the luminescence spectrum is not only dependent on the presence of defects and dopants but also on the particle size. Since only delocalized levels are affected by confinement, Co^{2+} *d*-band formation should lead to a size-dependent Co^{2+} luminescence feature. Knowledge of the electronic structure of Co^{2+} in ZnO may enhance the understanding of the mechanisms inducing high-temperature ferromagnetism. In addition to the luminescence measurements, the magnetic properties of aggregated ZnO nanocrystals containing different amounts of Co^{2+} were studied using SQUID magnetometry.

2. Experimental

2.1. Nanocrystal synthesis

Co^{2+} -doped ZnO nanocrystals were synthesized at room temperature using a wet chemical route as described by Schwartz et al. [8]. The precursor salts used are $\text{Zn}(\text{OAc})_2$ and $\text{Co}(\text{OAc})_2 \cdot 4\text{H}_2\text{O}$,

dissolved in DMSO. The total metal ion concentration in these solutions was kept at 0.1 M. Five millilitres of an 0.5 M ethanolic solution of $(\text{CH}_3)_4\text{NOH} \cdot 5\text{H}_2\text{O}$ (TMAH) is added dropwise to 15 ml of the dissolved metal salts. The nanocrystals can be washed and resuspended in ethanol as follows: first, the nanocrystals are precipitated from DMSO by adding 40 ml ethylacetate. After removing the supernatant, the crystals are resuspended in ethanol and washed again using a 2:1 mixture of heptane and ethylacetate. In a third washing step, pure heptane is used. Washing more than three times leads to irreversible aggregation of the nanocrystals. The washed suspensions are stable for several months.

2.2. Physical measurements

Room temperature steady-state luminescence spectra were taken using a FS920 luminescence spectrometer (Edinburgh Instruments). The different samples were measured in quartz cuvettes with a pathlength of 1.0 cm placed under an 45° angle with the incident beam. Fluorescence lifetime and low-temperature luminescence measurements were collected using an intensified CCD (Andor) attached to a Jarrel-Ash 0.5 m Ebert monochromator. A 337.1 nm pulsed nitrogen laser was used as the excitation source. Data acquisition by the CCD camera is triggered by the detection of the laser pulse using a laser diode. The samples were measured in a cylindrical quartz cuvette placed in a cryostat. Absorption spectra were collected with a Cary 500 UV–Vis–NIR spectrophotometer (Varian) using quartz cuvettes with a pathlength of 1 cm. Particle sizes were calculated from the shifts in energetic position of the band edge absorption using the equation proposed by Meulenkamp for pure ZnO [14].

The crystal structure of the nanocrystals was investigated using a Siemens D5000 X-ray diffractometer. The powders used for XRD were obtained by vacuum drying a three times washed sample at room temperature and heating up the remaining nanocrystals to 80°C for 15 min. Scanning electron micrographs and EDX data were taken using a FEI Quanta 200 F SEM combined with an EDAX-type Genesis 4000.

Dopant concentrations after synthesis were analytically determined using ICP-MS. Dry powder material obtained as above and dissolved in 1% HNO₃ was used for these measurements. Magnetic properties of the materials were measured using a Quantum Design MPMS-5S SQUID magnetometer. We used gelatin capsules as sample holders and their diamagnetic responses were removed from the measured magnetic moment.

3. Results and discussion

Fig. 1 shows an X-ray diffractogram of a dry nanocrystal powder. All the reflections could be assigned to the ZnO wurtzite structure giving a first indication that no Co related phases like CoO were formed in samples containing up to 10% Co. EDX and ICP-MS measurements indicated that the Co:Zn ratios found in the nanocrystals match those of the precursor solutions. ICP-MS data were indicative of very small amounts of Fe (0.01%).

Fig. 2 shows the absorption spectrum of a suspension of 2% Co²⁺:ZnO nanocrystals. It complies with previously reported spectra, featuring the ZnO exciton absorption at 330 nm and Co²⁺ absorption between 500 and 700 nm [15]. The former is shifted to shorter wavelengths relative to the bulk ZnO band gap (3.37 eV) absorption because of quantum confinement. The latter is related to a transition between the ⁴A₂

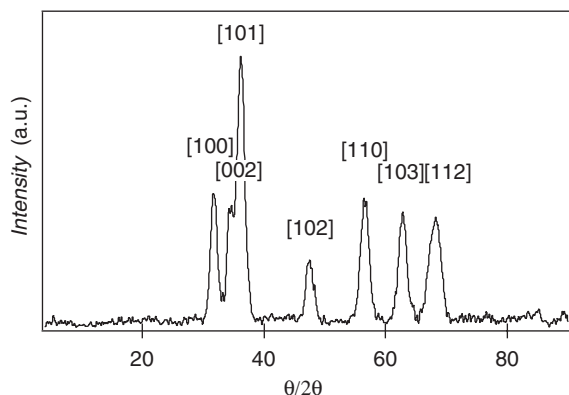


Fig. 1. XRD diffraction spectrum for 2% Co:ZnO powder.

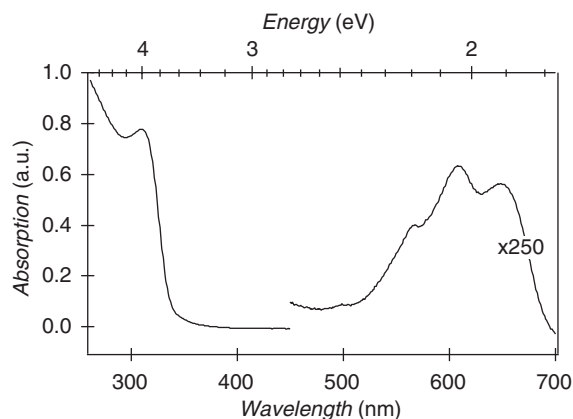


Fig. 2. Absorption spectrum of a suspension of 2% Co²⁺-doped ZnO nanocrystals taken 2 min after adding TMAH. On the left, the quantum confined band edge absorption is shown and on the right the Co²⁺ related absorption features.

ground state and the ⁴T₁(P) excited state of the Co²⁺ in the tetrahedral environment of the ZnO wurtzite lattice [15]. Its structure mainly arises from the spin orbit splitting of the ⁴T₁(P) state and to a minor extent from the mixing of this ⁴T₁(P) state with nearby spinforbidden doublet states (²E(G), ²T₁(G), ²A₁(G) and ²T₂(G)). The starting solution containing the original Co²⁺ ions in their octahedral environment is violet and turns blue on adding the TMAH, clearly indicating the environment of the Co²⁺ is changing and thus, the dopant ions are being included in the nanocrystals.

Fig. 3 represents two emission spectra of 2% Co:ZnO colloids. The spectra were taken respectively 5 and 370 min after initiation of particle growth. In this time interval, the mean particle diameter increases from 2.5 to 3.5 nm. As reported in the literature, both the exciton and the trap emission shift to lower energy with increasing particle size. As the yellow emission involves the trapping of a hole at the nanocrystal surface, its intensity is strongly reduced with decreasing surface-to-volume ratio [16]. The size dependence of the yellow emission is much smaller since the deep trap is a localized level originating from an oxygen vacancy which is not affected by quantum confinement. Increasing the Co²⁺ concentration to 10% results in an almost complete quenching of the yellow luminescence. Obviously, the presence

of Co^{2+} in the ZnO nanocrystals provides competitive pathways for recombination.

Next to the well-documented ZnO emission bands, a third emission feature at 1.8 eV is shown. This emission band shows a slight redshift relative to the Co^{2+} absorption. For low doped, bulk

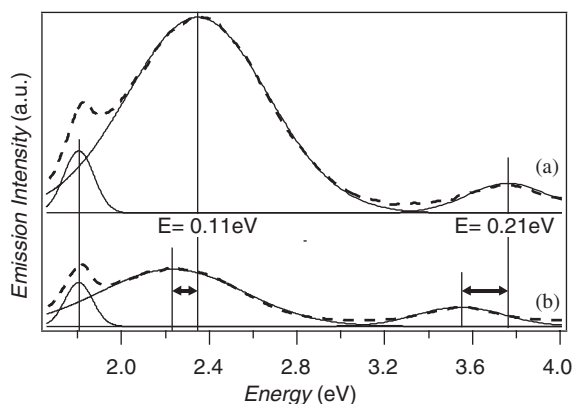


Fig. 3. Emission spectra ($\lambda_{\text{exc}} = 280 \text{ nm}$) of 2% Co^{2+} -doped ZnO colloids. Spectrum (a) was measured 5 min after initiating particle growth, spectrum (b) after 370 min. The three emission bands were fitted with a Gaussian line shape and the shifts in energetic position caused by particle growth are indicated in the figure.

$\text{Co}:\text{ZnO}$, an emission peak at 1.88 eV was interpreted as a mixed ${}^4\text{T}_1(\text{P}), {}^2\text{T}_1(\text{G}), {}^2\text{E}(\text{G}) \rightarrow {}^4\text{A}_2(\text{F})$ transition between cobalt d -levels incorporated in the ZnO host [17,18]. Given the correspondence between these data and our results, we conclude that the same interpretation holds for the additional emission at 1.8 eV. The emission associated with the Co^{2+} ions does not show a significant and systematic dependence on particle size (shift $< 0.01 \text{ eV}$). This indicates that it results from a transition between strongly localized Co^{2+} levels. As compared to the yellow emission, the intensity of the Co^{2+} related red emission does not decrease considerably upon particle growth, confirming the Co^{2+} emission is not a surface process originating from surface related levels. In addition, the spectral position and width of the emission is not influenced by changing the Co^{2+} concentration.

At 8 K, the Co^{2+} emission band appears as a superposition of the luminescence related to the internal Co^{2+} d -levels and a series of satellite peaks starting from 660 nm and decaying in intensity towards longer wavelengths (Fig. 4a). The energy splittings between the successive peaks match the literature data on the energies for E_2^{high} (0.055 eV) and E_2^{low} (0.012 eV) ZnO phonons [19].

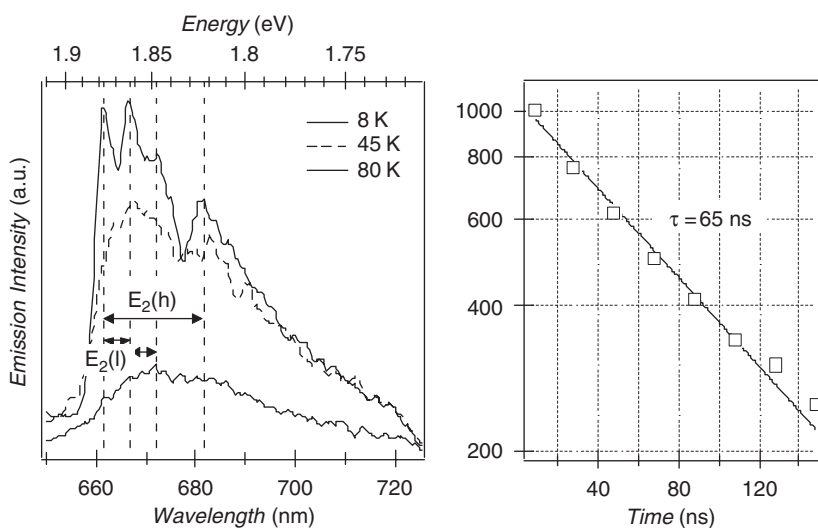


Fig. 4. (a) Low-temperature measurement for the Co^{2+} related emission. Below 60 K, phonon replicas from the ZnO lattice become visible. The energy differences between the small peaks are 0.054 eV for the $E_2(\text{h})$ phonon and 0.014 and 0.016 eV for the two $E_2(\text{l})$ phonon replicas which are in good agreement with the literature data. The particles were excited with laser light of 337 nm (3.69 eV). (b) Decay time curve for a 2% Co^{2+} -doped ZnO suspension measured at 14 K.

The presence of these bulk phonon replicas on the Co^{2+} emission clearly demonstrates that the Co^{2+} ions are indeed incorporated in the core of the nanocrystals instead of being adsorbed at the surface. At liquid nitrogen temperatures (80 K), these satellite peaks have completely disappeared. At 8 K as well as 77 K, the luminescence intensity of this red emission band has a lifetime of 65 ns (Fig. 4b).

Fig. 5 shows a set of excitation spectra obtained at different time intervals after initiating particle growth. Excitation of both the ZnO yellow emission ($\lambda_{\text{em}} = 530$ nm) and the Co^{2+} related emission ($\lambda_{\text{em}} = 680$ nm) shows a maximum coinciding with the ZnO band edge. The Co^{2+} related emission can also be excited at energies below the band edge. The intensity maximum at the band gap energy for the Co^{2+} emission results from the fact that the emission intensity measured at 680 nm is not only due to the emission coming from the Co^{2+} internal transitions but also from the visible emission which tails into this region as can be seen from the fits presented in Fig. 3. The energy shifts caused by particle growth are indicated in the excitation spectra (0.207 eV after 309 min) and are in good agreement with the energy shifts obtained from Fig. 3 (0.215 eV after 315 min). Excitation of

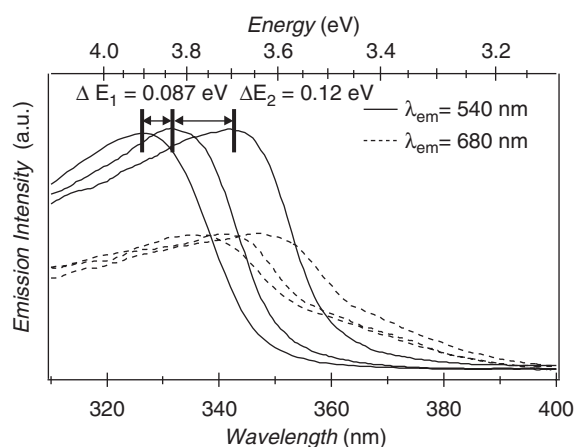


Fig. 5. Room temperature excitation spectra taken after different time intervals after initiating particle growth. For $\lambda_{\text{em}} = 530$ nm (full), after 8, 34, 317 min and for $\lambda_{\text{em}} = 680$ nm (dashed), after 10, 30, 305 min. Data for each set of measurements were normalized. For the $\lambda_{\text{em}} = 530$ nm data set, the energy shifts are indicated in the figure.

the Co^{2+} emission was not possible at wavelengths corresponding to the internal Co^{2+} absorption (500–700 nm).

Fig. 6 represents the results of SQUID measurements performed on dry powders. Since the precipitation from colloidal suspension and thermal treatment afterwards can play a major role in the magnetic properties of the final powders [8,13], samples were prepared using three different precipitation routes. The first sample was precipitated from suspension by drying at room temperature in vacuum. No subsequent heating steps were performed. The other two samples were precipitated by heating the suspensions up to 78 °C (boiling point of EtOH). Afterwards, one of these samples was heated to 120 °C during 1 h. All the samples showed paramagnetic behaviour at room temperature as well as at 40 K (Fig. 6). No significant differences between the different synthesis routes could be deduced. Using Curie's law, we calculate that, for the 1% samples, the measured paramagnetic susceptibility corresponds to an effective magnetic moment $\mu_{\text{eff}} = 3.85\mu_{\text{B}}/\text{Co}^{2+}$. This value agrees well with the expected effective magnetic moment of the $^4\text{A}_2$ ($S = 3/2$, $L = 0$) Co^{2+} ground state ($3.87\mu_{\text{B}}/\text{Co}^{2+}$). These results indicate that the mere introduction of Co^{2+} in the ZnO host is not sufficient to obtain room-temperature ferromagnetism or even d -band formation.

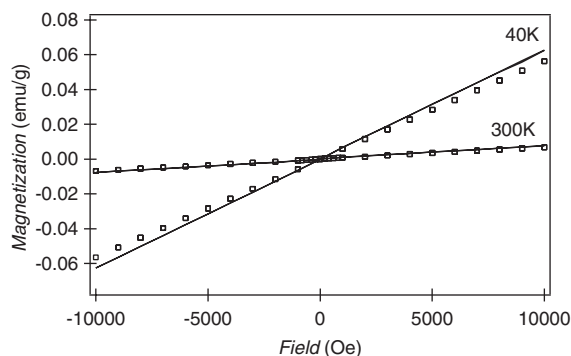


Fig. 6. Magnetic loops collected on 1% Co^{2+} powder samples at 40 and 300 K. Measurements were done on a sample dried at room temperature under vacuum (\square) and on a powder sample dried at 78 °C and treated in the furnace for 1 h at 120 °C (full line).

4. Conclusions

We characterized the luminescence of colloidal Co^{2+} -doped ZnO nanocrystals in order to relate the electronic properties of the material with its supposed ferromagnetic behaviour. The presence of Co^{2+} in the ZnO wurtzite host lattice leads to an additional emission band at 1.8 eV. At room temperature, no variation in terms of peak position and peak width of the Co^{2+} luminescence is observed by varying the diameter of the nanocrystals from 2.5 to 3.5 nm. In addition, the emission is not affected by changing the Co^{2+} concentration in the range 1–10%. At low temperature, the emission appears as a narrow line at the same energetic position as for bulk material, followed by well-resolved phonon replicas from the ZnO host. These data show that the Co^{2+} luminescence originates from strongly localized Co^{2+} levels, incorporated in the core of the nanocrystals. Indeed, on replacing one Zn^{2+} ion in 10 by a Co^{2+} ion, 1.67 hexagonal unit cells contain on the average one Co^{2+} ion. In that case, the average distance between Co^{2+} ions is 1.91 times the Zn–Zn bond length, i.e. 0.620 nm. Our measurements show that even then, electronic coupling between Co^{2+} ions is insufficient to affect the Co^{2+} luminescence. This strong localization of the Co^{2+} levels renders the hypothesis that formation of a Co^{2+} *d*-band leads to ferromagnetism in Co^{2+} -doped ZnO highly unlikely. The fact that neither ferromagnetism or a *d*-band was found in the Co^{2+} -doped ZnO nanocrystals leads to the conclusion that simple transition metal doping of ZnO semiconductor nanoparticles is insufficient to obtain ferromagnetism in these materials and suggests that further research on introducing defects leading to free charge carriers is necessary.

Acknowledgements

Z. Hens acknowledges Ghent University and the FWO-Vlaanderen for a research grant, P.F. Smet is a Research Assistant of the FWO-Vlaanderen.

References

- [1] S.A. Wolf, D.D. Awschalom, Science 294 (2001) 1488.
- [2] S.J. Pearton, D.P. Norton, K. Ip, Y.W. Heo, T. Steiner, Prog. Mater. Sci. 50 (2005) 293.
- [3] T. Dietl, H. Ohno, F. Matsukura, J. Cibert, D. Ferrand, Science 287 (2000) 1019.
- [4] H. Ohno, Science 281 (1998) 951.
- [5] T. Dietl, Semicond. Sci. Technol. 17 (2002) 377.
- [6] K. Sato, H. Katayama-Yoshida, Semicond. Sci. Technol. 17 (2002) 367.
- [7] M. Vanketsan, C.B. Fitzgerald, J.G. Lunney, J.M.D. Coey, Phys. Rev. Lett. 93 (2004) Art. no. 177206.
- [8] D.A. Schwartz, N.S. Norberg, Q.P. Nguyen, J.M. Parker, D.R. Gamelin, J. Am. Chem. Soc. 125 (2003) 13205.
- [9] K. Ando, H. Saito, Z. Jin, T. Fukumara, M. Kawasaki, Y. Matsumoto, H. Koinuma, J. Appl. Phys. 89 (2001) 7284.
- [10] W. Prellier, A. Fouchet, C. Simon, B. Mercey, Mater. Sci. Eng. B-Solid State Mater. Adv. Technol. 109 (2004) 192.
- [11] N. Jedrecy, H.J. von Bardeleben, Y. Zheng, J.L. Cantin, Phys. Rev. B 69 (2004) Art. no. 041308.
- [12] D.A. Schwartz, D.R. Gamelin, Adv. Mater. 16 (2004) 2115.
- [13] K.R. Kittilstved, N.S. Norberg, D.R. Gamelin, Phys. Rev. Lett. 94 (2005) Art. no. 147209.
- [14] E.A. Meulenkamp, J. Phys. Chem. B 102 (1998) 5566.
- [15] H.A. Weakliem, J. Chem. Phys. 36 (1962) 2117.
- [16] A. van Dijken, E.A. Meulenkamp, D. Vanmaekelbergh, A. Meijerink, J. Lumin. 90 (2000) 123.
- [17] H.-J. Schulz, M. Thiede, Phys. Rev. B 35 (1987) 18.
- [18] P. Koidl, Phys. Rev. B 15 (1977) 2493.
- [19] C.A. Arguello, D.L. Rousseau, S.P.S. Porto, Phys. Rev. 181 (1969) 1351.